Characterization and Transport Properties of Nafion/Polyaniline Composite Membranes

Sophie Tan and Daniel Bélanger*

Département de Chimie, Université du Québec à Montréal, Case Postale 8888, succursale Centre-Ville, Montréal, Québec, Canada H3C 3P8

Received: August 22, 2005; In Final Form: September 28, 2005

Nafion membranes were modified by chemical polymerization of aniline using ammonium peroxodisulfate as the oxidant. The Nafion−polyaniline composite membranes were extensively characterized using scanning electron microscopy (SEM), atomic force microscopy (AFM), infrared (FTIR-ATR) and X-ray photoelectron spectroscopy (XPS), thermogravimetric analysis (TGA), differential scanning calorimetry (DSC), and ion-exchange capacity measurements. The transport properties were also evaluated by conductivity and electrodialysis measurements. The data show that when a high oxidant concentration (1 M $(NH_4)_2S_2O_8$) is used, polyaniline is mostly formed at the surface of the Nafion membrane with a higher proportion of oligomers. On the contrary, when 0.1 M oxidant is used, polyaniline is mostly formed inside the ionic domains of Nafion, blocking the pathway to ion transport and thus reducing the transport of Zn^{2+} as well as the transport of H^+. These data were also compared to the data obtained with poly(styrene sulfonate)−PANI composite membranes.

Introduction

Perfluorinated ionomer-based polymers have been studied since the late 1970s and early 1980s with the commercialization of Nafion membranes from DuPont. These membranes were first used in the chlor−alkali industry for electrodialysis processes. The structure of Nafion is illustrated below. It is composed mainly of a PTFE backbone with side-chains containing ether groups and a sulfonic acid unit at its end. Nowadays, perfluorinated membranes are extensively studied for their applications in fuel cells, particularly, for direct methanol fuel cells. To date, Nafion is still the most performing cation-exchange membrane due to its high chemical and mechanical stability as well as its good proton conductivity.[1] However, some progress is still needed in order to enhance the membrane performance in terms of permselectivity, water management, and stability at high temperatures. For this reason, researchers have synthesized new polymeric membranes derived from the perfluorosulfonic acid structure or containing fluorine backbones.[2,3] Others have studied the modification of Nafion membranes using inorganic fillers such as SiO_2,[4,5] mordenite,[6] inorganic acids,[7,8] a polymer coating and/or filler such as poly(vinyl alcohol),[9] poly(1-vinylimidazole),[10] and poly(vinylidene fluoride).[11] Nafion has also been modified with conducting polymers such as poly(pyrrole)[12−16] and poly(aniline) (PANI)[17] to reduce the methanol crossover in direct methanol fuel cell applications. Sata et al.[18] have briefly mentioned the use of perfluorocarbon sulfonic acid modified with polypyrrole for electrodialysis applications. Nevertheless, very few teams have studied the Nafion−PANI composite membranes. Nafion−PANI composites have been studied mostly for electrode modifications in order to mix the electronic conductivity of PANI and the ionic conductivity of Nafion.[19−23]

Prior to this work, we have demonstrated the possibility of improving the permselectivity of poly(styrene sulfonic acid) membranes for the transport of protons against bivalent cations (Zn^{2+} and Cu^{2+}) by modifying these membranes with a thin layer of polyaniline.[24,25] It was also shown that the permselectivity behavior was linked to the location of the PANI layer within the membrane matrix.[26]

SCHEME 1: Structure of Nafion

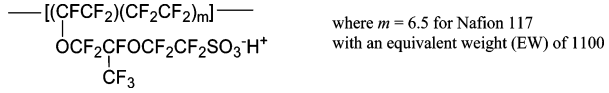

The aim of this work is to study the modification of Nafion 117 membranes by in-situ chemical polymerization of aniline. More specifically, the Nafion−PANI membrane will be extensively characterized using several techniques in order to understand how the microstructure of this composite membrane affects its transport properties in electrodialysis applications.

Experimental Section

Materials and Chemicals. HCl (EMD), H_2SO_4 (EMD), NaCl (BDH), $(NH_4)_2S_2O_8$ (BDH), and $ZnSO_4 \cdot 7H_2O$ (Anachemia) were of ACS reagent grade and used as received. Aniline (Acros) was distilled twice prior to use. Millipore water (18 MΩ·cm obtained from a Sybron/Barnstead Nanopure system) was used for the preparation of all solutions. The perfluorosulfonate cation-exchange membrane used in this study was the Nafion 117 (DuPont). The membrane was pretreated by boiling in H_2O_2 (3% v/v), H_2O, H_2SO_4 (0.5 M), and H_2O for 1 h and stored in 1 M HCl.

Membrane Modification with Polyaniline. The Nafion membranes were conditioned in 1 M HCl for more than 24 h prior to modification. The modification was carried out in two steps at room temperature in a Teflon two-compartment cell (surface-modified: 9.6 cm^2). The first step consisted of exchanging the protons in the membrane with protonated aniline, that is, anilinium ions, by adding, in one compartment, 40 mL of 1 M aniline solution in 1 M HCl, and water in the second compartment. After rinsing with water, the aniline solution was replaced by 40 mL of 1 or 0.1 M $(NH_4)_2S_2O_8$ solution. This second step polymerizes the anilinium species exchange within the membrane. The two-step method allows modification on a

* Corresponding author. E-mail: belanger.daniel@uqam.ca.

10.1021/jp054724e CCC: $30.25
Published on Web 11/18/2005

single face of the membrane. The modified membranes were stored either in 1 M HCl or 1 M H_2SO_4 solutions. The membrane identification is as follows: Naf PX-Y-Z where P stands for polyaniline, X represents the time (h) used in the exchange of anilinium ions, Y is the reaction time (h), and Z is the concentration (M) of the oxidant.

Instrumental Characterization. For all instrumental techniques, membranes were conditioned in 1 M HCl. When required, membranes were dried under vacuum for at least 36 h at room temperature in the presence of P_2O_5.

Atomic force microscopy (AFM) images were recorded in the tapping mode using a Nanoscope III Dimension 3100 AFM instrument (Digital Instruments) with an etched silicon aluminum coated tip. Samples were only partially dried with a nitrogen flow to remove surface water. Scanning electron microscopy (SEM) micrographs were taken using a Hitachi model S-4300E/N scanning electron microscope with dried samples. SEM samples were sputtered with gold to reduce charging effects during measurements.

The Fourrier transform infrared (FTIR) spectra were recorded using a Thermo-Nicolet Nexus 870 spectrometer equipped with a mercury cadmium telluride (MCTA) detector and a ZnSe attenuated total reflection (ATR) platform. The spectra shown are obtained with dried samples using 128 scans at a resolution of 4 cm^{-1}.

XPS analyses were performed using a VG Escalab 220i-XL system equipped with a hemispherical analyzer and an Al anode (Kα X-rays at 1486.6 eV) used at 10 kV and 15 mA. The data were recorded at room temperature and at a pressure below 10^{-6} Pa. To compensate for charging effects, binding energies were corrected for covalent C1s at 284.6 eV after curve fitting. Curve fitting and peak integration were carried out using the CasaXPS (version 2.1.25) software. After a Shirley background correction, all peaks were fitted by assuming a Gaussian−Lorentzian line shape. The surface atomic composition was calculated using the high-resolution spectra and the appropriate relative sensitivity factors: C1s (1.00), F1s (4.43), N1s (1.80), O1s (2.93), $Cl2p_{1/2}$ (0.775), $Cl2p_{3/2}$ (1.51), $S2p_{1/2}$ (0.567), and $S2p_{3/2}$ (1.11).

Thermogravimetric (TGA) and differential scanning calorimetry (DSC) measurements were done with wet samples from which excess water was removed by wiping the membranes using a filter paper. The TGA thermograms were recorded using a Seiko Exstar 6200 TG/DTA and the DSC thermograms, with a TA Instrument 2910 DSC equipped with a liquid nitrogen cooling accessory (LNCA).

Ion-Exchange Capacity (IEC). All membranes were washed and stabilized in 1 M HCl, H_2O, and 1 M NaCl alternatively for 1 h in each solution during 3 cycles. The membranes are then soaked for 24 h in a 1 M NaCl solution to ion-exchange H^+ with Na^+. After removing excess sodium chloride (by immersion in water for 30 min and rinsing with water), the membranes were dried under vacuum at room temperature for at least 36 h over P_2O_5 before being weighed. The Na^+ ions were ion-exchanged with H^+ by immersion in a 1 M HCl solution for 24 h. The sodium concentration in the latter solution was determined by atomic absorption spectroscopy (Varian SpectrAA 220FS).

Water Uptake. The membranes were washed, stabilized, and conditioned in 1 M HCl as for IEC measurements. After removing excess chloride by immersion in water and rinsing with water, the membranes were blot dried with a filter paper and weighed immediately. Then, the membranes were dried (under vacuum at room temperature for at least 36 h over P_2O_5) and weighed again. The water uptake (% H_2O) was determined according to the following equation:

$$\%\ H_2O = \frac{m_{\text{wetmembrane}} - m_{\text{drymembrane}}}{m_{\text{drymembrane}}} \times 100 \qquad (1)$$

where m is the mass (g).

Electrodialysis. Electrodialyses were performed in a two-compartment cell containing, in the anodic compartment, 150 mL of 1.5 g/L Zn in 0.5 M H_2SO_4 and in the cathodic compartment, 33 mL of 0.5 M H_2SO_4. The modified surface, that is, the surface exposed to the oxidant, (surface area: 5.1 cm^2) was placed facing the anolyte unless otherwise specified. A current density of 100 mA/cm^2 was applied between two platinum plates (surface area: ~7.5 cm^2) for 3 h using a M273 potentiostat/galvanostat (EG & G Princeton Applied Research). The electrodialysis was carried out under a nitrogen flow. The metal concentration in both compartments was determined by atomic absorption spectroscopy (Varian SpectrAA 220FS). From these concentrations, the % Zn^{2+} leakage is calculated according to the following equation:

$$\%\ Zn^{2+}\ \text{leakage} = \frac{m_{Zn^{2+}}(\text{catholyte})}{m_{Zn^{2+}}(\text{catholyte}) + m_{Zn^{2+}}(\text{anolyte})} \times 100 \qquad (2)$$

Conductivity Measurements. Measurements were carried out at room temperature (23 ± 1) °C in 0.5 M H_2SO_4 using a two-compartment cell containing 150 mL of solution each and separated by the cation-exchange membrane (effective area: 0.44 cm^2) with the modified surface (exposed to the oxidant) facing the anodic compartment. Membranes were conditioned in 0.5 M H_2SO_4 for at least 24 h prior to measurements. The electrical current was applied between two platinum electrodes using the galvanodynamic mode at 1 μA/s, and the open-circuit voltage was measured between two Ag/AgCl (3 M KCl) reference electrodes placed on each side of the membrane at a distance of 4 mm from its surface. The instrument used to apply the current and measure the open-circuit voltage was a Solartron 1470 battery test unit. The conductivity values were calculated from the slope of the current−voltage curves and using a membrane thickness of 170 μm. The solution resistance was measured using the same setup and its value was subtracted to the total resistance value measured, before calculating the membrane conductivity.

Results

Chemical Polymerization of Aniline on Nafion. In this work, polymerization is carried out in a two-compartment cell to favor polymerization on a single face of the membrane. In fact, a minimal quantity of PANI is wanted on the membrane in order to block transport of bivalent cations and, in the meantime, maintaining good ionic conductivity. After exchanging the Nafion counterions (H^+) with anilinium ions (protonated aniline), the cell was rinsed several times with water before replacing the aniline solution by the peroxodisulfate ammonium solution ($(NH_4)_2S_2O_8$), the oxidant. Concentrations of 0.1 and 1.0 M oxidant were studied. When using the 1 M oxidant solution, polymerization takes place quite rapidly, but a visually homogeneous and dark PANI layer is obtained after 1 h of polymerization (Naf P1-1-1). Over 1 h of polymerization, the PANI layer is visually similar, but the blocking behavior of the membrane for Zn^{2+} is lost, most likely due to the degradation of PANI.[24] With 0.1 M $(NH_4)_2S_2O_8$, a transparent but homo-

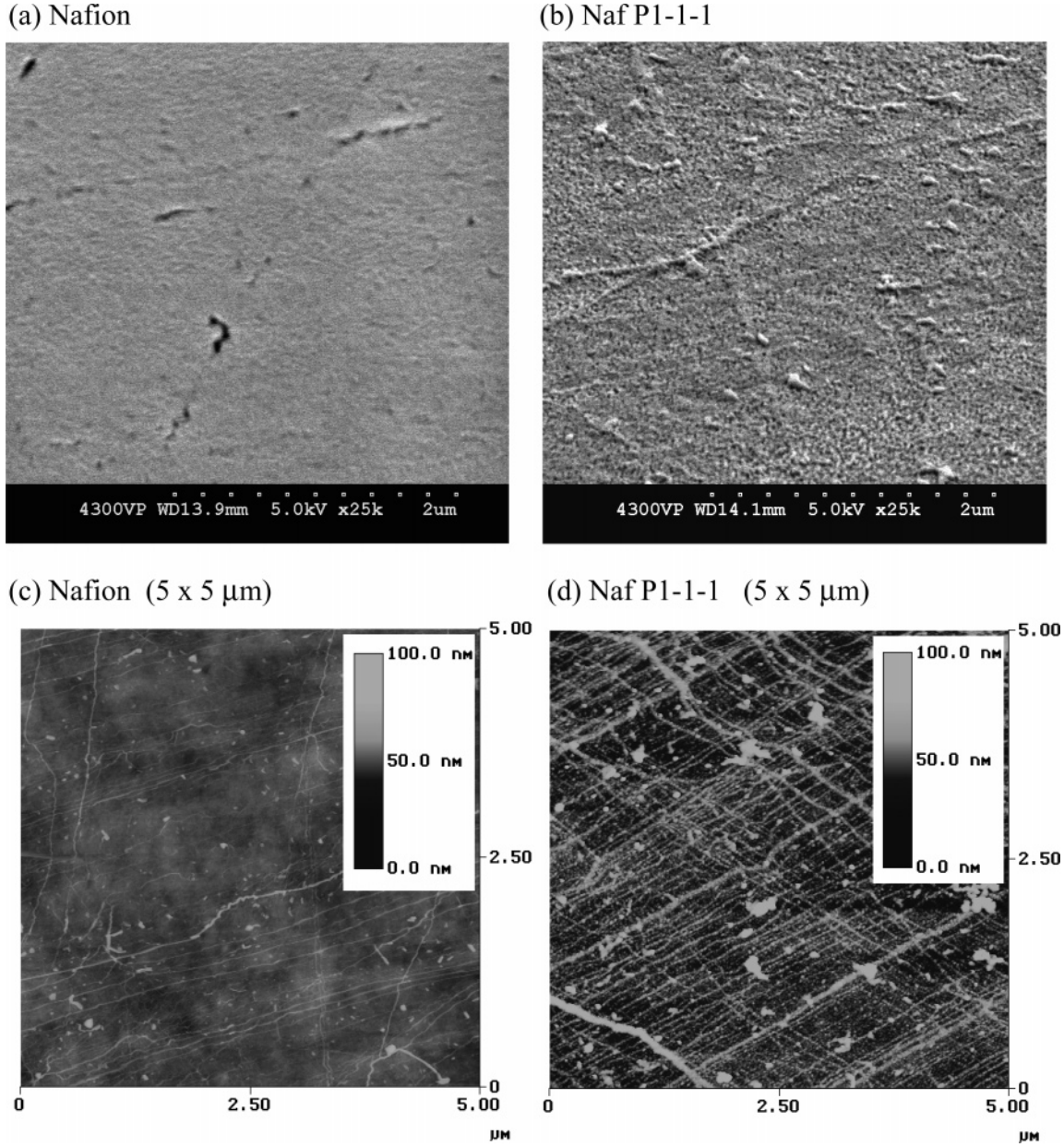

Figure 1. SEM images of (a) Nafion 117 and (b) Naf P1-1-1 (bar scale represents 2 μm) and AFM images of (c) Nafion 117 and (d) Naf P1-1-1.

geneous PANI layer is obtained after 1 h of oxidation. Yet, only the membrane prepared with a 2-h oxidation time (Naf P1-2-0.1) yielded in a good blocking behavior toward Zn^{2+} ions (see below). Therefore, only the Naf P1-1-1 and Naf P1-2-0.1 were characterized and presented in this article. Visually, both composite membranes exhibit the same dark blue color. However, it should be mentioned that after 1 h of oxidation using 1 M $(NH_4)_2S_2O_8$, a yellow-brown precipitate is found in the water compartment, opposite to the compartment containing the oxidant. This precipitate has the characteristic color of benzoquinone, the degradation product of PANI following hydrolysis.[24,27,28] Also, after storage of Naf P1-1-1 in 1 M HCl or H_2SO_4 for over 24 h, a pink color appears on the unmodified surface of the membrane around the modified area. At longer storage times, the aqueous solution also becomes pink. The pink color was not observed in the case of Naf P1-2-0.1, even over two months of storage in acid solutions (1 M HCl). These observations suggest that the use of 1 M $(NH_4)_2S_2O_8$ can lead to the presence of oligomers on the Naf P1-1-1 membrane, which can diffuse through the membrane.

SEM and AFM. Figure 1, parts a and b, present the SEM surface micrographs of the bare Nafion and Naf P1-1-1 membranes. After modification, a change in surface topography is observable. The PANI coating seems to be heterogeneous, displaying some aggregates along with some fibril-like structures. However, one should be very careful in attributing the surface features solely to the presence of PANI, particularly for images obtained by SEM at high magnification factors. It was observed that the Nafion surface topography tends to change during image acquisition due to burning and degradation of the surface, even with a gold coating added to minimize surface charging effects. For example, Figure 1a shows some cracks at the surface of Nafion which appear during image acquisition. These cracks are formed most likely due to water removal from the surface and burning effects. The formation of holes on Nafion was also observed during irradiation with Ga^+ ions using the focused ion-beam technique (known as FIB).[29] Nevertheless, some coating is apparent at the surface of the modified membranes.

The membrane topography can also be monitored by atomic force microscopy. The advantage of AFM (tapping mode) over SEM is that AFM can probe the surface of the membrane without using a radiation source that can burn the surface and without adding a gold layer which could slightly alter the topography of the membrane. In addition, AFM imaging can be performed in a partially dried state, whereas the conventional SEM technique used in this work requires drier samples. Drying can also introduce changes in the surface morphology of the polymers, as mentioned above.

AFM images of the unmodified and modified Nafion (Naf P1-1-1) are presented in Figure 1, parts c and d. Comparison of Figure 1, parts c and d, depicts some similar features such as the presence of linear and particulate structures. The linear structure found on the Nafion surface is most likely caused by the extrusion procedure used in the preparation of the Nafion commercial membrane.[30,31] Despite the similarities found on the surface of both membranes, Figure 1d shows that the modification enhances these defects at the surface of Nafion, suggesting that polymerization occurs primarily at surface imperfections of the membranes. However, the density of polyaniline fibrils seems to be larger than the density of linear surface imperfections, but the entire surface is not covered by PANI. Interestingly, the fibril-like structure of PANI was also observed by Wen and Kocherginsky[32] for polyaniline membranes doped with 1 M HCl, such as in the case of the membranes presented in Figure 1.

The differences observed between Figure 1, parts b and d, can be attributed to the drying state of the membrane as well as the fact that SEM can alter the surface of the Nafion membrane after irradiation. It should also be noted that SEM probes a few micrometers depth and the image acquired is actually an image of the first few micrometers of the membrane. In contrast, the AFM technique probes the surface with a depth in the order of nanometers (100 nm in this case). The PANI fibril-like structure is possibly present only at the surface of the membrane.

FTIR-ATR Spectroscopy. The FTIR-ATR spectrum of Nafion, Naf P1-2-0.1, and Naf P1-1-1 are shown in Figure 2a. The characteristic infrared bands and their assignation for the unmodified Nafion[16,33,34] are presented in Table 1. The first noticeable difference between Nafion and Nafion−PANI membranes is the absence of the band associated with the H_3O^+ species at around 1710 cm^{-1} in the case of Nafion−PANI membranes. This suggests that the Nafion−PANI membranes are less hydrophilic than bare Nafion, since all membranes were dried under the same conditions. Second, the presence of polyaniline at the surface of a Nafion membrane can be observed by the appearance of additional bands at around 1584 and 1493 cm^{-1} both on Naf P1-2-0.1 and Naf P1-1-1 membranes. These bands can be, respectively, attributed to the quinoid and benzenoid stretching modes of polyaniline.[35−38] The relative intensities of these bands are indicative of the proportion of quinoid and benzenoid units. For instance, Naf P1-1-1 seems to have around 50% of each unit whereas Naf P1-2-0.1 contains a larger proportion of benzenoid units, which suggests that PANI on Naf P1-1-1 is more oxidized than on Naf P1-2-0.1. This could be expected since Naf P1-1-1 was prepared using a higher oxidant concentration.

Other characteristic bands for the PANI emeraldine form (protonated by HCl) are usually found at around 1306, 1250, and 1140 cm^{-1} assigned to C−N stretching, $C-N^{\bullet+}$ stretching, and $-NH^+=$ stretching, respectively.[35] These bands are not observable on Naf P1-1-1 due to the small amount of PANI detected at its surface, quinoid (1580 cm^{-1}) and benzenoid (1500 cm^{-1}) bands being weak. For Naf P1-2-0.1, which seems to contain a larger amount of PANI at its surface, additional features can be observed when comparing the Nafion and Naf P1-2-0.1 spectra in Figure 2a. The band at 1302 cm^{-1} appears more intense and wider, suggesting the presence of the C−N stretching band associated with PANI. Similarly, bands associated with the positively charged components of PANI at 1250 and 1140 cm^{-1} are most likely superimposed on the broad CF_2 band between 1300 and 1100 cm^{-1}, since the latter band is wider than the one corresponding to Nafion.

From the infrared spectra, it is also possible to retrieve information on ionic interactions between the SO_3^- groups and the PANI positively charged groups. The SO_3^- symmetric stretching band (1057 cm^{-1}) can shift when a change in polarization of the S−O dipole is induced by its ionic environ-

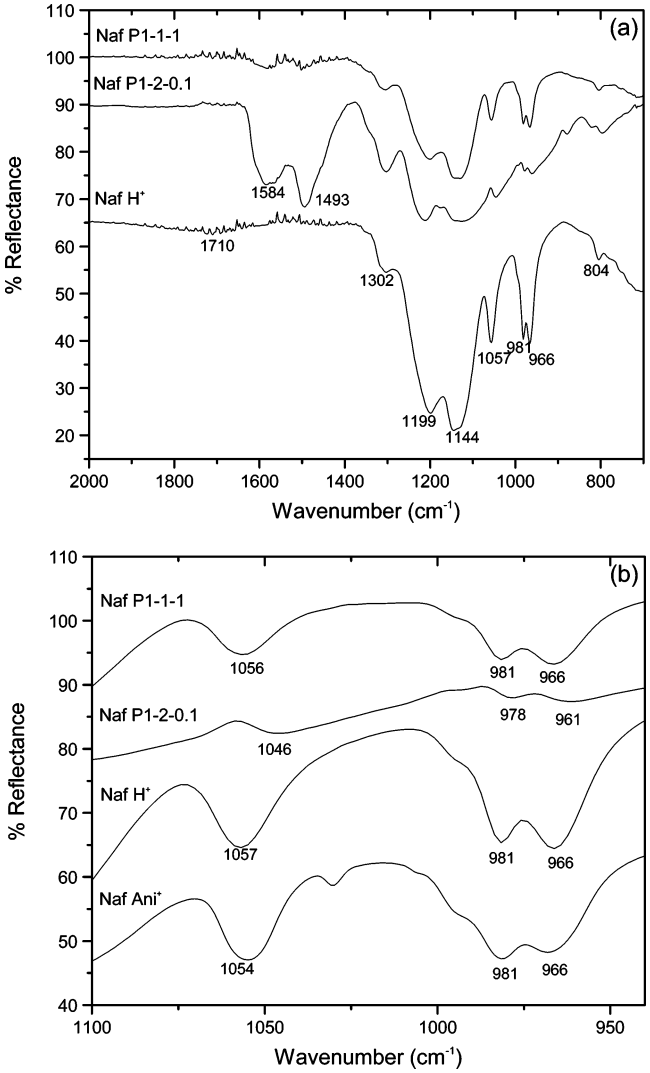

Figure 2. FTIR-ATR spectra of Naf P1-1-1, Naf P1-2-0.1, Nafion 117 in its protonated form (Naf H^+), and Nafion exchanged with anilinium ions (Naf Ani^+): (a) spectral region between 700 and 2000 cm^{-1}, and (b) between 900 and 1100 cm^{-1}.

TABLE 1: FTIR Characteristic Bands of Nafion 117

frequency (cm^{-1})	assignment
1500−2050	hydrated H_3O^+
1199	CF_2 asymmetric stretching
1144	CF_2 symmetric stretching
1057	SO_3^- symmetric stretching
981 & 966	C−O−C stretching
804	C−S stretching

TABLE 2: Surface Atomic Composition Determined by XPS

	%C								
	C−C, C−H	C−F	% F	% O	% S	% N	% Cl	N^+/N	Cl^-/N
Naf	5.4	29.6	55.9	6.1	1.4	0	0		
Naf P1-2-0.1	39.3	19.3	29.4	5.7	0.8	4.8	1.0	0.30	0.20
Naf P1-1-1	65.9	8.3	7.1	12.2	0.3	7.3	1.5	0.48	0.20

ment. Lowry and Mauritz[39] have demonstrated that the SO_3^- stretching band decreases from 1073 to 1057 cm^{-1} as the radius of the monovalent cation increases (with Li^+, Na^+, K^+, Rb^+). However, according to the same authors, this shift is observed only when Nafion contains very little water (below 7 wt %). Similarly, Lage et al.[40] have noted a shift of the SO_3^- band toward lower values with bivalent cations (Ca^{2+}, Sr^{2+}, and Ba^{2+}). The shift in the SO_3^- stretching band has also been observed in the case of ionic interactions between SO_3^- groups and positively charged polymers. Tannenbaum et al.[41] have observed the SO_3^- band shift from 1059 cm^{-1} for Nafion to 1052 cm^{-1} for Nafion in the presence of a poly(ethylacrylate-*co*-4-vinylpyridine). They explained this shift by a lower polarization of the S−O dipole due to an increased separation between SO_3^- and H^+ following proton transfer between the sulfonate groups and positively charged pyridine units.

Figure 2b illustrates an enlargement of the spectral region showing the SO_3^- stretching band. It can be seen that the stretching band shifts from 1057 cm^{-1} for Nafion (Naf H^+) to 1056 cm^{-1} for Naf P1-1-1 and 1046 cm^{-1} for Naf P1-2-0.1. In the case of Naf P1-1-1, a very little shift occurs, most likely due to the small amount of PANI found at the surface of the membrane. Nevertheless, this is consistent with the band displacement observed by Park et al.[16] for the interactions between polypyrrole and the Nafion SO_3^- groups. Figure 2b includes the corresponding infrared spectrum for Nafion exchanged with anilinium ions (Naf Ani^+). The latter shows that, as for PANI, anilinium ion interactions with SO_3^- groups decrease the frequency of its stretching band following a weaker polarization of the S−O bond. For Naf P1-2-0.1, a more important shift toward lower values is observed, suggesting that a large amount of positively charged groups are interacting with the SO_3^- groups.

Surface Chemical Composition by XPS. The elemental composition determined by XPS for all membranes is given in Table 2. The C1s core level spectra of the unmodified and modified membranes are presented in Figure 3a. The peak envelope first shows the presence of at least two components mainly attributed to the C−C and C−H environment at low binding energy and the C−F environment at high binding energy. In fact, the C1s peak can be fitted with at least five components which are detailed in Table 3 and Figure 3a. The resulting peak components are consistent with those previously reported by Huang et al.[42] After modification of the membrane, the low binding energy component increases and the C−F component decreases, indicating that polyaniline is present at the surface and partially covering the Nafion membrane, as observed by the SEM and AFM images. The C−N component of PANI can be detected at (285.5 ± 0.3) eV after curve fitting.[43]

The polyaniline layer can be characterized by the N1s high-resolution spectra, illustrated in Figure 3b for both composite membranes. The N1s peak can be fitted with at least three components found at 399.6, 400.8, and 402.3 eV, the first peak being attributed to −NH− and the two last peaks to positively charged nitrogen.[26,43−45] Since the composite membranes have been conditioned in 1 M HCl prior to the XPS analysis, polyaniline is expected to be in its positively charged form. As indicated in Table 2, the N^+/N ratio was found to be higher for Naf P1-1-1 than for Naf P1-2-0.1 which is consistent with the FTIR-ATR results of the quinoid/benzenoid ratio observed in Figure 2a. Actually, the protonation of the imines ($-NH^+=$) present in the PANI chains is more favorable than for the amine groups ($-NH_2^+-$) since its pK_a value is 5.5 compared to 2.5 for the amine groups. Therefore, the higher the quinoid/benzenoid ratio, the higher the N^+/N ratio will be. These data indicate once more that the PANI found on Naf P1-1-1 is more oxidized and contains more oligomers than Naf P1-2-0.1.

The presence of the dopant, chloride ions, can also be detected at a binding energy of around 200 eV (not shown). The Cl^-/N ratio was found to be 0.20 both for Naf P1-2-0.1 and Naf P1-1-1 membranes (Table 2). This ratio is slightly lower than the value usually found for the emeraldine form of PANI, that is, 0.30.[46] On the other hand, since the polymerization was performed in or at the surface of Nafion, a portion of the positively charged imines or amines can be compensated by $-SO_3^-$ groups. Indeed, when comparing the S2p spectrum of the unmodified membrane to the S2p spectra (Figure 3c) of the modified membranes, a shift in binding energy is observed toward lower values in the presence of PANI. The lower binding energy values suggest the presence of interactions between the $-SO_3^-$ and $=NH^+-$ or $-NH_2^+-$ functional groups.[24,45,47] A similar observation was noted for poly(styrene sulfonate) membranes modified with polyaniline,[24] and this is consistent with the FTIR results. Figure 3c also shows that the presence of a PANI layer at the surface of the membrane covers the Nafion sulfonate groups, lowering the S2p intensity, as was observed for the F1s and C1s peaks. It should be noted that in contrast to the FTIR results, XPS data suggest that more PANI is found at the surface of Naf P1-1-1 membrane than for Naf P1-2-0.1. This apparent contradiction is most likely related to the depth of analysis for both spectroscopic techniques. In fact, XPS probes only 5 to 10 nm depth whereas FTIR-ATR allows the detection of chemical species found in the first few microns.

The unmodified Nafion O1s high-resolution spectrum (Figure 3d) exhibits two peaks centered at 533.0 and 535.3 eV attributable to sulfonic acid oxygen and ether oxygen, respectively.[48,49] With the presence of PANI, the O1s peak shape changes and the overall atomic percentage increases (Table 2). This was unexpected since no oxygen atom is present in PANI and the O1s peak intensity was expected to be lowered as for sulfur and fluorine. Curve fitting of the O1s peaks reveals the appearance of two new components in the presence of PANI. First, a peak appears at 534.1 eV which could be attributed to the sulfonate oxygen compensated by the charged imine (or amine) groups from PANI. As observed in the S2p spectra of Nafion−PANI composite membranes, the presence of charged imine groups allows stabilization of the negative charge on the sulfonate group which decreases the electron density around the oxygen atom and increases the electron density around the sulfur atom.[24,45,47] In the case of sulfur, it was previously mentioned that the presence of PANI lowers the S2p peak binding energy following the increase in electron density around the sulfur atom. In the same manner, oxygen from the sulfonate groups would possess a higher binding energy in the presence

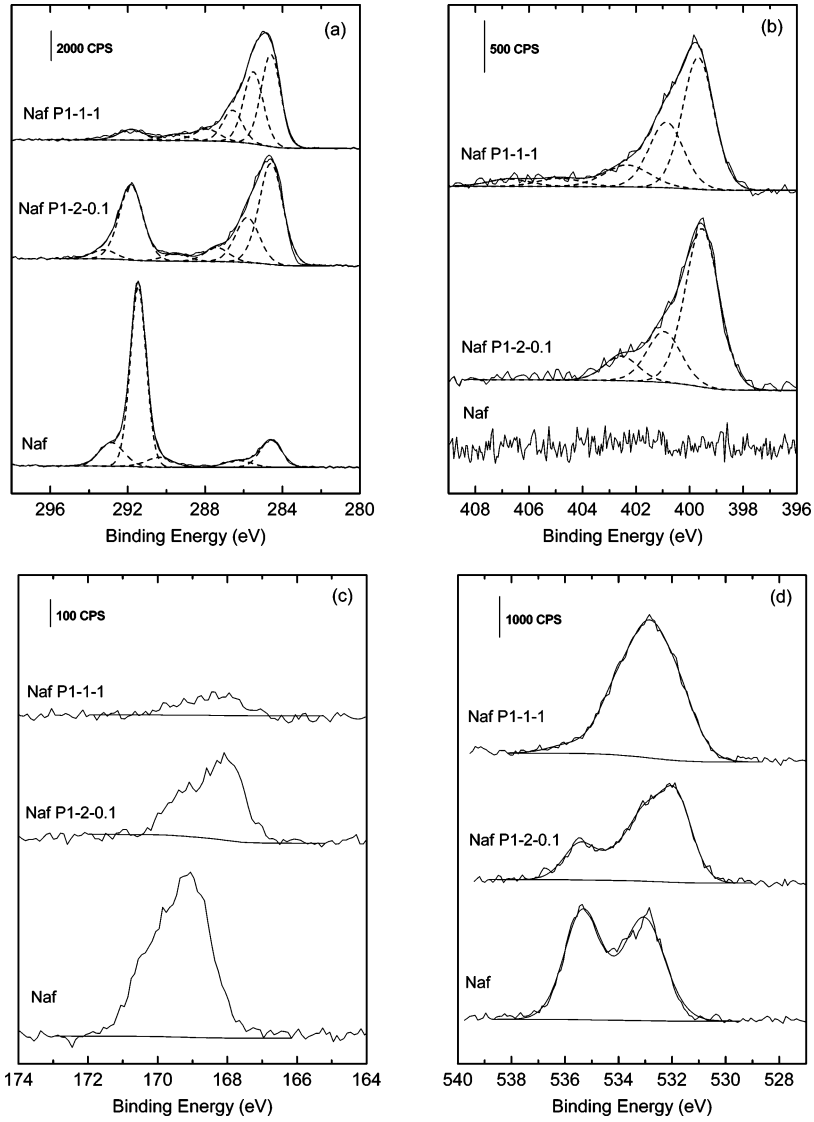

Figure 3. High-resolution XPS spectra of the surface of Nafion and Nafion−PANI membranes: (a) C1s, (b) N1s, (c) S2p, and (d) O1s.

TABLE 3: Curve Fitted C1s Core Level Spectrum Components for Nafion

peak position (eV)	fwhm (eV)	area (CPS*eV)	% of total C	assignment
284.6	1.3	2633	13.2	C−C
286.3	1.6	817	4.1	C−O
290.4	1.6	1151	5.8	?
291.5	1.0	12651	63.4	CF_2, CF−O
292.8	1.5	2579	13.0	CF_3

of positively charged groups. Second, Figure 3d illustrates the appearance of an additional peak at lower binding energy centered at 531.8 eV. We believe that this peak can be attributed to bicarbonate (HCO_3^-) adsorbed on PANI. In fact, George et al.[50] have characterized the $-NH_3^+HCO_3^-$ compound using XPS by the following peaks: 531.9 eV for the O1s in HCO_3^- and 288.8 eV for the C1s in HCO_3^-. When fitting the C1s spectra of Nafion−PANI membranes, a peak is found at approximately 289.3 eV. This suggests that polyaniline does adsorb carbon dioxide in the presence of air and water forming HCO_3^- species. Carbon dioxide adsorption occurred although the composite membranes were dried under vacuum after their preparation (the overall sample exposition to air was less than 1 h), indicating that the $-NH_3^+HCO_3^-$ interaction is quite strong.

Thermogravimetric Analysis. The thermal stability of the Nafion−PANI composite membranes in comparison to the bare Nafion was studied by TGA under air atmosphere. According to the literature, thermogravimetric (TG) curves recorded under N_2 atmosphere are characterized by four phases: (i) gradual loss of water from 25 to ∼290 °C, (ii) desulfonation (with the loss of SO_2) combined with the decomposition of the ether groups (C−O−C) on the side-chains, between 290 and 400 °C, (iii) side-chain decomposition at 400 to 470 °C, and (iv) decomposition of the poly(tetrafluoroethylene) backbone at 470 to 560 °C.[51,52] Figure 4 illustrates the TG and differential thermogravimetric (DTG) curves of Nafion, Naf P1-1-1 and Naf P1-2-0.1 recorded under air atmosphere. The Nafion DTG curve (Figure 4b) exhibits transitions at the temperature ranges of 25−250 °C, 290−390 °C, 390−475 °C, and 475−545 °C which are in concordance with the four decomposition stages given in the literature and described above. Only the PTFE backbone decomposition occurs at a lower temperature range due to the presence of air. After polymerization of aniline on Nafion membranes, it can first be observed that the modified membranes contain less water (18%) than the bare Nafion (23%) and this is consistent with the FTIR-ATR spectra (Figure 2a) showing that the presence of PANI decreases the hydrophilicity of the membrane. Second, the Nafion−PANI membrane DTG

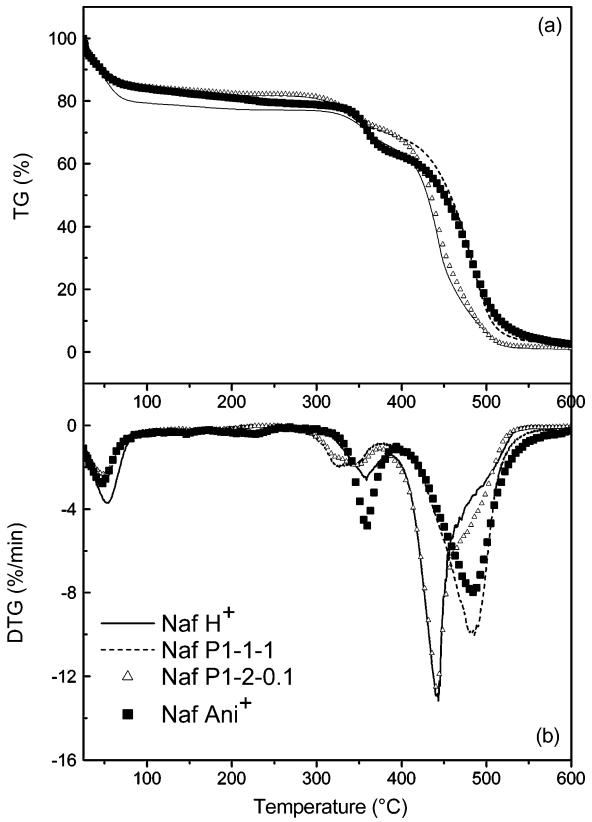

Figure 4. Thermogravimetric analysis curves of Nafion 117 in its protonated form (Naf H^+), Naf P1-1-1, Naf P1-2-0.1, and Nafion exchanged with anilinium ions (Naf Ani^+) recorded under air atmosphere at 10 °C/min: (a) TG (%) and (b) DTG (%/min).

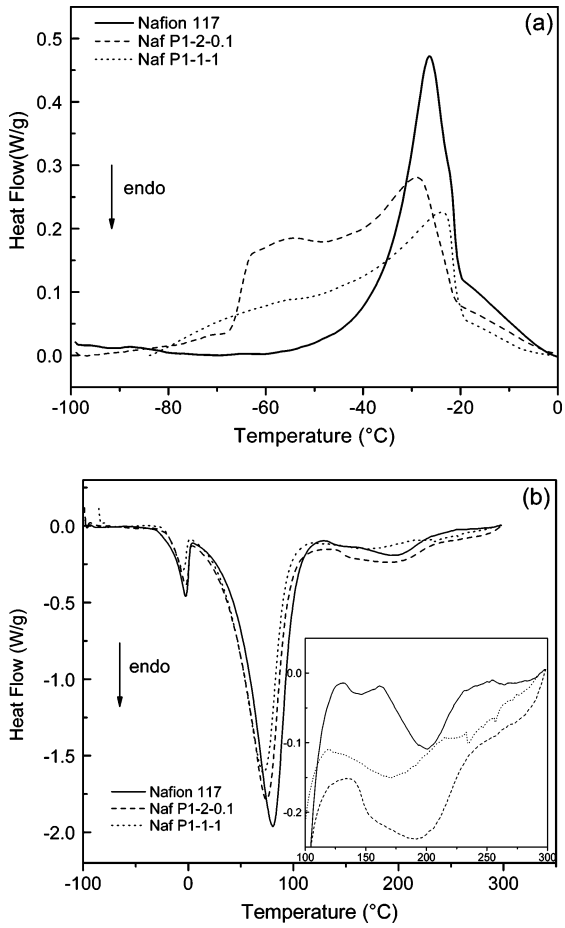

Figure 5. DSC first cooling (a) and heating (b) curves of Nafion 117, Naf P1-2-0.1 and Naf P1-1-1 membranes. The inset is an expansion of the region between 100 and 300 °C. Measurements were recorded under helium atmosphere.

curve indicates that the degradation of the sulfonate groups starts at a lower temperature than for the bare Nafion and seems to occur in two stages, according to Figure 4b. The first stage starts at 265 °C for both membranes, and the second stage starts at around 335 °C for Naf P1-1-1 and 325 °C for Naf P1-2-0.1. The two different stages could be attributed on one hand to SO_3^- and C−O−C decomposition occurring in the presence or absence of PANI. On the other hand, the two stages could also be associated with the SO_3^- interacting with PANI and the C−O−C decomposition occurring separately. Actually, the weight percent (wt %) lost up to the temperature between both peaks corresponds approximately to the wt % associated with sulfur when calculated with the IEC values, and this supports the latter hypothesis. Nonetheless, care should be taken in the interpretation of the decomposition stages since they do not necessarily occur separately, and different functional groups can degrade simultaneously. As for the side-chains and backbone decomposition of the Nafion−PANI membranes, it occurs in the same temperature range for Naf P1-2-0.1, as opposed to Naf P1-1-1, for which it is shifted to higher temperatures. The difference between both Nafion−PANI composite membranes could be related to the chain length of PANI and/or to the location of the PANI chains within the Nafion matrix. Indeed, Nafion exchanged with anilinium ions ($C_6H_5-NH_3^+$), identified as Naf-Ani^+, also exhibits this shift toward higher temperature for the side-chains and backbone degradation (Figure 4b). Rollet et al.[53] have previously demonstrated that ammonium ions tend to diffuse in the intermediate phase of Nafion composed of ether side-chains. Thus, if most of the PANI chains found in the Naf P1-1-1 are located in the intermediate phase with the positively charged groups oriented toward the sulfonic acid clusters, as it would be for anilinium ions, then it could change the morphology and thermal stability of these side-chains. This would explain the shift toward higher temperatures observed in the degradation of the side-chains for both Naf-Ani^+ and Naf P1-1-1. Hence, Naf P1-1-1 could contain a large amount of oligomers which would have similar interactions with the Nafion membrane as the anilinium ions and thus, leading to a similar Nafion morphology. In fact, the presence oligomers in Naf P1-1-1 was previously evidenced by the observation of a pink coloration around the modified area of the membrane, the higher quinoid/ benzenoid and N^+/N ratios.

Differential Scanning Calorimetry. DSC thermograms of Nafion can reveal information about the states of water found in the membrane as well as the SO_3^- cluster transitions. First, it is known that three different states of water are generally found in ionomers such as Nafion membranes: (i) unbound freezable water, (ii) bound freezable water, and (ii) unfreezable water.[54,55] The unbound freezable water behaves much like bulk water and is not interacting with the polymer; the bound freezable water is the water found inside the pores or clusters of the polymer but not strongly associated with the polymer contrarily to unfreezable water, which would be strongly associated with the polymer and for which it is not possible to observe the crystallization and melting transitions. Figure 5a shows the first cooling curves obtained with the Nafion and Nafion−PANI composite membranes. Nafion presents an exothermic peak at around −20 °C associated with the crystallization of water. This crystallization temperature is in concordance with values published by other researchers.[56,57] Since the crystallization temperature is below 0 °C, it can be qualified as bound freezable

TABLE 4: Membrane Physical Properties and Transport Behavior

	Zn^{2+} leakage (%) ±0.5	σ (mS/cm)	IEC (mmol/g)	water updake (wt %) ±1	PANI (wt %) ±1
Nafion	11	136	0.93 ± 0.04	33	
Naf P1-2-0.1	<0.5	6.5	0.90 ± 0.08	31	2.7
Naf P1-1-1	5	65.2	0.78 ± 0.04	28	3.3

water. This supercooling effect has been reported in the literature with different hydrophilic polymers, such as cellulose and hydroxymethacrylates derivatives,[54,58] and is caused by the interactions of the water molecules with the hydrophilic units or ionic sites.

Water in Naf P1-1-1 composite membranes seems to behave in the same manner as for the unmodified Nafion since water freezes at approximately the same temperature but over a wider range. The effect of PANI is more important in the case of Naf P1-2-0.1 where the peak is clearly split in two. This splitting was previously observed by Saito et al.[57] and Asaka et al.[55] for different perfluorosulfonic acid membranes exchanged with various counterions. They have explained this splitting by the presence of different states of water. In addition, Asaka et al. have suggested that the freezable bound water is actually found in the ionic clusters of Nafion. Thus, if the latter hypothesis is true, it could imply that Naf P1-2-0.1 contains PANI chains or aggregates inside the ionic clusters which would affect the state of water present, resulting in a split crystallization peak.

Regarding the heating curves, the peak maxima for the melting and vaporization of freezable water are observed at around −5 and 70 °C, respectively (Figure 5b). The vaporization temperature is the same as the one obtained by TGA (Figure 4b). In addition, the region above 100 °C shows two endothermic peaks interpreted as a cluster transition at 146 °C and melting of the non polar crystallite backbone at 200 °C.[59] Once modified, the cluster transition temperature of Nafion increases whereas the melting temperature decreases. These tendencies are consistent with those observed by Park et al. for Nafion membranes modified with polypyrrole.[16] It is plausible to assume that the presence of PANI forces the Nafion polymer chains to re-organize themselves and form a more cross-linked structure within the clusters which would increase the cluster transition temperature.

Membrane Transport Properties. As mentioned in the Introduction, the main objective in modifying the Nafion membranes with polyaniline is to block the transport of Zn^{2+} during electrodialysis in acidic media. Therefore, to evaluate the blocking behavior of the Nafion−PANI composite membranes toward bivalent cations, electrodialysis assays using a two-compartment cell were performed. Table 4 gives the zinc leakage percentage obtained for the unmodified and modified membranes. The membrane modification with polyaniline seems to improve its blocking behavior for the transport of Zn^{2+}, since after modification the Zn leakage drops from 11 to 5% for Naf P1-1-1 and to < 0.5% for Naf P1-2-0.1. However, the decrease in Zn^{2+} leakage is associated with a loss in ionic conductivity, and in fact the ionic conductivity decreases proportionally with the Zn^{2+} leakage. This loss in conductivity has been previously reported by several teams working on the modification of Nafion for reducing the methanol crossover in direct methanol fuel cells.[13,16,17] The linear relationship between zinc leakage and ionic conductivity could suggest that PANI chains are partially blocking the ionic cluster network by reducing the number of ion-exchange sites. Indeed, some interactions exist between the positively charged PANI chains and the sulfonate groups, as demonstrated by the FTIR-ATR, XPS, DSC, and TGA results described above. On the other hand, Table 4 shows that the IEC value for Naf P1-1-1 is lower than for Naf P1-2-0.1 while the conductivity of the latter is significantly lower. The weight increase associated with the amount of PANI, which is only slightly higher for Naf P1-1-1 than for Naf P1-2-0.1 (Table 4), cannot explain why the Naf P1-1-1 IEC value is much lower. An explanation for this contradictory result is proposed below. Table 4 also shows that the water uptake decreases with the small increase in the amount of PANI, which is consistent with the FTIR-ATR and TGA results.

Discussion

Microstructure of Nafion−PANI Composite Membranes. To better understand the relationship between the presence of PANI in Nafion and the transport properties of the composite membranes, it would be useful to try to determine the location of PANI within the structure of Nafion. Nafion is structurally composed of three regions: (i) the poly(tetrafluoroethylene) backbone which is very hydrophobic; (ii) the hydrophilic ionic sites (SO_3^-), and (iii) an intermediate region containing the ether side-chains. Several studies have been reported on the morphology of Nafion since the early 1980s. Mauritz and Moore have recently published a complete review on the models describing the morphology of Nafion.[30] Among others, there is the well-known cluster−network model, developed by Gierke et al.[60,61] in 1982, suggesting the presence of hydrophilic ionic clusters linked together by ionic channels, which allow the transport of ions, in a hydrophobic matrix. Since then, other models have been suggested such as the core−shell structure with an ion-rich core (Fujimura et al.[62]), the hard sphere model (Kumar and Pineri,[63] Orfino and Holdcroft[64]), and the lamellar model (Litt[65]). In more recent years, studies tend to suggest that the ionic sites are grouped together in rodlike or ribbonlike structures and that these ionic aggregates might be linked together by only one SO_3^- group instead of channels.[30] Up to now, the morphology of Nafion is still not completely elucidated, and there is not a general agreement on the Nafion structure. Nevertheless, it is generally agreed that the ionic sites can reorganize themselves depending on the hydration level of the polymer. It is also known that there is a hydrophilic path through which water and ions are transported.

The modification of Nafion membranes by in-situ polymerization of aniline will certainly affect the microstructure of the membrane. For instance, it is believed that a portion of the PANI chains are present in the hydrophilic clusters since the ionic transport is partially inhibited. However, the two Nafion−PANI composite membranes seem to present different microstructures as well as physical and transport properties. First, XPS data suggest that Naf P1-1-1 has more PANI at its surface than Naf P1-2-0.1. On the other hand, FTIR-ATR data demonstrate the opposite but, as explained earlier, this is probably due to the difference in depth of analysis between XPS and FTIR-ATR. In addition, the different results obtained with these two surface techniques suggests that the PANI layer in Naf P1-1-1

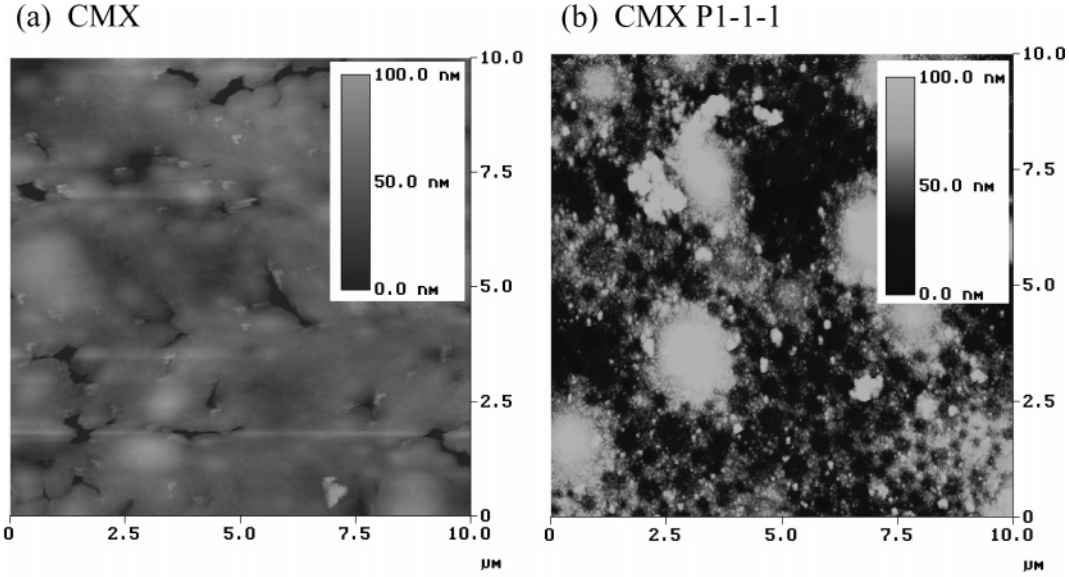

Figure 6. AFM images of (a) unmodified CMX and (b) PANI-modified CMX membranes.

is most likely found at the surface of the membrane with less than 1 μm of thickness within the Nafion membrane. Second, FTIR-ATR, DSC, electrodialysis, and conductivity results suggest that Naf P1-2-0.1 contains more PANI inside the ionic clusters. The difference between both Nafion−PANI composite membranes is most likely related to the polymerization conditions. In the case of Naf P1-1-1, the high oxidant concentration (1 M) and short reaction time (1 h) would favor the relatively fast polymerization of aniline at the surface of the Nafion membrane. Zawodzinski et al.[66] have demonstrated by contact angle measurements that when Nafion is in contact with liquid water, a high concentration of SO_3^- groups are at the interface of Nafion and water; however, when in contact with saturated vapor water, the surface is rich in fluorinated carbon chains. Hence, when protons are exchanged with anilinium ions, during the first step of the modification, anilinium ions can be found at the surface. Upon addition of the oxidant, polymerization will first occur at the surface. Moreover, the negative charge of the oxidant, $S_2O_8^{2-}$ will most likely keep the oxidant from diffusing through the Nafion cation-exchange membrane, resulting in the formation of PANI at the surface of Nafion. In contrast, Naf P1-2-0.1 is prepared using a low oxidant concentration (0.1 M) and a longer reaction time (2 h). The low concentration of oxidant would slow the polymerization process, allowing the oxidant to penetrate inside the membrane through the hydrophilic channels or path as the positively charged PANI chains are formed in the hydrophilic ionic clusters. It is also possible to imagine that the $-SO_3-\cdots{}^+H_3N-C_6H_5$ ionic pair is reorientated toward the bulk of the membrane as the polymerization proceeds to favor the interactions of the PANI chains with the intermediate phase, which would be thermodynamically favorable. Indeed, the PANI chains could be located either in the intermediate region between the hydrophobic and the hydrophilic region, as was demonstrated by small-angle neutron scattering measurements for $N(CH_3)_4^+$ ions,[53] or in the hydrophilic clusters.

The observed differences in morphology between both Nafion−PANI composite membranes could explain why the IEC of Naf P1-1-1 is lower than the IEC of Naf P1-2-0.1 despite the fact that it does not block as efficiently the transport of cations. In fact, to completely block the transport of cations through the membrane, it is only necessary to disrupt all the channels through which the ions are transported. Thus, if the PANI chains are mostly formed in the channels, such as in the case of Naf P1-2-0.1, it is possible that they simply block more ion transport channels than Naf P1-1-1. The latter probably contains about the same amount or maybe a little more PANI chains or oligomers than Naf P1-2-0.1 (Table 4), but PANI is present mostly at the surface of the membrane without blocking entirely the ion channels. Furthermore, Naf P1-1-1 contains more short chains or oligomers of PANI, as evidenced by the higher quinoid/benzoid and N^+/N ratios obtained by FTIR-ATR and XPS, respectively. These short chains could also diffuse inside the membranes and reduce the IEC of the membrane without totally blocking the transport of cations. The latter hypothesis was also suggested to explain the relatively high decomposition temperature of the Nafion side-chains observed by TGA.

Comparison with Poly(styrene sulfonate)−PANI Composite Membranes. In our previous work, we have characterized the poly(styrene sulfonate)-polyaniline composite membranes prepared in a similar fashion.[24−26] Thus, it could be interesting to compare the physical and ion transport properties of these composite membranes with those of the Nafion-polyaniline membranes. The first observation made during the modification of the membranes is that it is much more difficult to obtain a uniform and thin PANI layer on the Nafion membrane. For example, a Nafion-PANI membrane prepared using a 1 h oxidation time and a 0.1 M $(NH_4)_2S_2O_8$ solution as the oxidizing agent (Naf P1-1-0.1), which had a transparent green color, did not present any significant blocking behavior toward Zn^{2+} ions (10% Zn leakage). In addition, although a dark PANI layer is obtained, as in the case of Naf P1-1-1 and Naf P1-2-0.1, SEM (Figure 1) and XPS (Figure 3) results show that a total coverage of the surface of Nafion cannot be obtained. In contrast, visually transparent and uniform layers of PANI can be formed at the surface of Neosepta CMX membranes as previously reported.[26] At a smaller scale, the AFM images represented in Figure 6b also show that the PANI morphology is porous as opposed to the fibril-like structure obtained on Nafion and shown in Figure 1d. The difference in the nature of the substrate certainly has an impact on the nature of the layer at the surface of the composite membranes. The perfluorocarbon chains of Nafion are very hydrophobic as compared to anilinium species and do not contain any phenyl rings that could have provided some kind of π-stacking interactions such as in the case of polystyrene sulfonate substrates.[24,26]

Another point of interest is to compare how the presence of PANI affects the membrane permselectivity for protons against Zn^{2+}. In the present work, the results suggest that the composite membrane having the best blocking behavior is the membrane containing PANI in the ionic clusters which interrupts the ionic path through the membrane. In contrast, it was previously demonstrated for the CMX−PANI composite membrane that only a very thin but uniform layer of PANI at the surface of the membrane is required to block efficiently the transport of Zn^{2+} without significantly decreasing the proton conductivity.[24−26] The differences observed between both types of composite membranes with respect to the transport property behavior can be explained by the morphology of the polymer membrane itself. As described above, Nafion is known to phase separately into hydrophobic and hydrophilic regions with an intermediate phase containing the ether side-chains. Thus, ions are most likely being transported through the ionic channels or ionic clusters. The phase separation of the ionic species explains why Nafion has a high ionic conductivity when compared to that of other ionomers. Poly(styrene sulfonate) possesses a more rigid structure and does not allow the sulfonic acid groups to reorganize themselves into a separate phase. For this reason, sulfonic acid groups are probably more randomly dispersed through the polymer of the CMX membrane.

Conclusion

To summarize, the main goal of this work was to characterize the Nafion−PANI composite membranes in order to get a better understanding of the Nafion microstructure after modification with polyaniline. From the data obtained, we believe that, depending on the polymerization conditions, it is possible to prepare a Nafion−PANI composite membrane with shorter PANI chains mainly found in the intermediate phase of Nafion (with high oxidant concentration and short polymerization time) and a composite membrane with longer PANI chains mostly found inside the ionic clusters or channels (with low oxidant concentration and longer polymerization time). In addition, it is demonstrated that the ionic transport of both H^+ and Zn^{2+} will be dependent on the amount of polyaniline disrupting the ionic paths and not necessarily the total amount of PANI. The amount of PANI found in the ionic paths area would in turn depend on the chain length of PANI and the polymerization conditions. Hence, this study gives an insight on how the presence of polyaniline could affect the Nafion morphology and transport properties. It could contribute to the understanding of the factors involved in the ionic transport through Nafion membranes and in the development of cation-exchange membranes for fuel cells.

Acknowledgment. This research was funded by the Natural Science and Engineering Research Council of Canada through a strategic grant (234959-00) and an equipment grant for an XPS spectrometer (to D.B. and nine others). The authors would like to thank Prof. Julian Zhu (Université de Montréal) for the use of his DSC instrument, Prof. Mario Morin (UQÀM) for his FTIR-ATR instrument, Patricia Moraille (Université de Montréal) for her help on the AFM, and Raymond Mineau (UQÀM) for taking the SEM micrographs. S.T. acknowledges the Natural Science and Engineering Research Council of Canada and the "Fonds Québécois de Recherche sur la Nature et les Technologies" for graduate student fellowships. The financial contribution of UQAM is also acknowledged.

Supporting Information Available: Pictures of modified membranes obtained under different polymerization conditions are provided. This material is available free of charge via the Internet at http://pubs.acs.org.

References and Notes

(1) Smitha, B.; Sridhar, S.; Khan, A. A. *J. Membr. Sci.* **2005**, *259*, 10.
(2) Li, Q. F.; He, R. H.; Jensen, J. O.; Bjerrum, N. J. *Chem. Mater.* **2003**, *15*, 4896.
(3) Nasef, M. M.; Saidi, H.; Yarmo, M. A. *J. New Mater. Electrochem. Syst.* **2000**, *3*, 309.
(4) Miyake, N.; Wainright, J. S.; Savinell, R. F. *J. Electrochem. Soc.* **2001**, *148*, A905.
(5) Baradie, B.; Dodelet, J. P.; Guay, D. *J. Electroanal. Chem.* **2000**, *489*, 101.
(6) Kwak, S. H.; Yang, T. H.; Kim, C. S.; Yoon, K. H. *Solid State Ionics* **2003**, *160*, 309.
(7) Malhotra, S.; Datta, R. *J. Electrochem. Soc.* **1997**, *144*, L23.
(8) Dimitrova, P.; Friedrich, K. A.; Stimming, U.; Vogt, B. *Solid State Ionics* **2002**, *150*, 115.
(9) Shao, Z. G.; Hsing, I. M. *Electrochem. Solid State Lett.* **2002**, *5*, A185.
(10) Bae, B. C.; Ha, H. Y.; Kim, D. *J. Electrochem. Soc.* **2005**, *152*, A1366.
(11) Song, M. K.; Kim, Y. T.; Fenton, J. M.; Kunz, H. R.; Rhee, H. W. *J. Power Sources* **2003**, *117*, 14.
(12) Easton, E. B.; Langsdorf, B. L.; Hughes, J. A.; Sultan, J.; Qi, Z. G.; Kaufman, A.; Pickup, P. G. *J. Electrochem. Soc.* **2003**, *150*, C735.
(13) Langsdorf, B. L.; Sultan, J.; Pickup, P. G. *J. Phys. Chem. B* **2003**, *107*, 8412.
(14) Langsdorf, B. L.; MacLean, B. J.; Halfyard, J. E.; Hughes, J. A.; Pickup, P. G. *J. Phys. Chem. B* **2003**, *107*, 2480.
(15) Smit, M. A.; Ocampo, A. L.; Espinosa-Medina, M. A.; Sebastian, P. J. *J. Power Sources* **2003**, *124*, 59.
(16) Park, H. S.; Kim, Y. J.; Hong, W. H.; Choi, Y. S.; Lee, H. K. *Macromolecules* **2005**, *38*, 2289.
(17) Shimizu, T.; Naruhashi, T.; Momma, T.; Osaka, T. *Electrochemistry* **2002**, *70*, 991.
(18) Sata, T.; Funakoshi, T.; Akai, K. *Macromolecules* **1996**, *29*, 4029.
(19) Andreev, V. N.; Zolotarevskii, V. I. *Russ. J. Electrochem.* **2005**, *41*, 189.
(20) Li, N.; Lee, J. Y.; Ong, L. H. *J. Appl. Electrochem.* **1992**, *22*, 512.
(21) Barthet, C.; Guglielmi, M. *Electrochim. Acta* **1996**, *41*, 2791.
(22) Aldebert, P.; Audebert, P.; Armand, M.; Bidan, G.; Pineri, M. *J. Chem. Soc., Chem. Commun.* **1986**, 1636.
(23) Orata, D.; Buttry, D. A. *J. Electroanal. Chem.* **1988**, *257*, 71.
(24) Tan, S.; Laforgue, A.; Bélanger, D. *Langmuir* **2003**, *19*, 744.
(25) Tan, S.; Viau, V.; Cugnod, D.; Bélanger, D. *Electrochem. Solid State Lett.* **2002**, *5*, E55.
(26) Tan, S.; Tieu, J. H.; Bélanger, D. *J. Phys. Chem. B* **2005**, *109*, 14085.
(27) Angelopoulos, M.; Asturias, G. E.; Ermer, S. P.; Ray, A.; Scherr, E. M.; MacDiarmid, A. G.; Akhtar, M.; Kiss, Z.; Epstein, A. J. *Mol. Cryst. Liquid Cryst.* **1988**, *160*, 151.
(28) Stilwell, D. E.; Park, S. M. *J. Electrochem. Soc.* **1988**, *135*, 2497.
(29) Park, Y. S.; Yamazaki, Y. *Solid State Ionics* **2005**, *176*, 1079.
(30) Mauritz, K. A.; Moore, R. B. *Chem. Rev.* **2004**, *104*, 4535.
(31) James, P. J.; McMaster, T. J.; Newton, J. M.; Miles, M. J. *Polymer* **2000**, *41*, 4223.
(32) Wen, L.; Kocherginsky, N. M. *Synth. Met.* **1999**, *106*, 19.
(33) Shao, Z. G.; Joghee, P.; Hsing, I. M. *J. Membr. Sci.* **2004**, *229*, 43.
(34) Gruger, A.; Regis, A.; Schmatko, T.; Colomban, P. *Vib. Spectrosc.* **2001**, *26*, 215.
(35) Trchova, M.; Sedenkova, I.; Tobolkova, E.; Stejskal, J. *Polym. Degrad. Stabil.* **2004**, *86*, 179.
(36) Stejskal, J.; Trchova, M.; Prokes, J.; Sapurina, I. *Chem. Mater.* **2001**, *13*, 4083.
(37) Varela, H.; Torresi, R. M.; Buttry, D. A. *J. Braz. Chem. Soc.* **2000**, *11*, 32.
(38) Kang, E. T.; Neoh, K. G.; Tan, K. L. *Prog. Polym. Sci.* **1998**, *23*, 277.
(39) Lowry, S. R.; Mauritz, K. A. *J. Am. Chem. Soc.* **1980**, *102*, 4665.
(40) Lage, L. G.; Delgado, P. G.; Kawano, Y. *Eur. Polym. J.* **2004**, *40*, 1309.
(41) Tannenbaum, R.; Rajagopalan, M.; Eisenberg, A. *J. Polym. Sci. Pt. B−Polym. Phys.* **2003**, *41*, 1814.
(42) Huang, C. D.; Tan, K. S.; Lin, H. Y.; Tan, K. L. *Chem. Phys. Lett.* **2003**, *371*, 80.
(43) Chen, Y.; Kang, E. T.; Neoh, K. G.; Lim, S. L.; Ma, Z. H.; Tan, K. L. *Colloid Polym. Sci.* **2001**, *279*, 73.
(44) Neoh, K. G.; Kang, E. T.; Tan, K. L. *J. Phys. Chem. B* **1997**, *101*, 726.
(45) Wei, X. L.; Fahlman, M.; Epstein, K. J. *Macromolecules* **1999**, *32*, 3114.

(46) Neoh, K. G.; Kang, E. T.; Tan, K. L. *J. Phys. Chem.* **1991**, *95*, 10151.
(47) Goh, S. H.; Lee, S. Y.; Zhou, X.; Tan, K. L. *Macromolecules* **1998**, *31*, 4260.
(48) Schulze, M.; Lorenz, M.; Wagner, N.; Gulzow, E. *Fresenius J. Anal. Chem.* **1999**, *365*, 106.
(49) Susac, D.; Kono, M.; Wong, K. C.; Mitchell, K. A. R. *Appl. Surf. Sci.* **2001**, *174*, 43.
(50) George, I.; Viel, P.; Bureau, C.; Suski, J.; Lecayon, G. *Surf. Interface Anal.* **1996**, *24*, 774.
(51) de Almeida, S. H.; Kawano, Y. *J. Therm. Anal. Calorim.* **1999**, *58*, 569.
(52) Nagarale, R. K.; Gohil, G. S.; Shahi, V. K.; Rangarajan, R. *Macromolecules* **2004**, *37*, 10023.
(53) Rollet, A. L.; Diat, O.; Gebel, G. *J. Phys. Chem. B* **2002**, *106*, 3033.
(54) Hatakeyama, H.; Hatakeyama, T. *Thermochim. Acta* **1998**, *308*, 3.
(55) Asaka, K.; Fujiwara, N.; Oguro, K.; Onishi, K.; Sewa, S. *J. Electroanal. Chem.* **2001**, *505*, 24.
(56) Laporta, M.; Pegoraro, M.; Zanderighi, L. *Phys. Chem. Chem. Phys.* **1999**, *1*, 4619.
(57) Saito, M.; Hayamizu, K.; Okada, T. *J. Phys. Chem. B* **2005**, *109*, 3112.
(58) Gates, G.; Harmon, J. P.; Ors, J.; Benz, P. *Polymer* **2003**, *44*, 215.
(59) Stefanithis, I. D.; Mauritz, K. A. *Macromolecules* **1990**, *23*, 2397.
(60) Hsu, W. Y.; Gierke, T. D. *J. Membr. Sci.* **1983**, *13*, 307.
(61) Hsu, W. Y.; Gierke, T. D. *J. Electrochem. Soc.* **1982**, *129*, C121.
(62) Fujimura, M.; Hashimoto, T.; Kawai, H. *Macromolecules* **1982**, *15*(5), 136.
(63) Kumar, S.; Pineri, M. *J. Polym. Sci., Pt. B—Polym. Phys.* **1986**, *24*, 1767.
(64) Orfino, F. P.; Holdcroft, S. *J. New Mater. Electrochem. Syst.* **2000**, *3*, 285.
(65) Litt, M. *Abstr. Pap. Am. Chem. Soc.* **1997**, *213*, 33-POLY.
(66) Zawodzinski, T. A.; Shoichet, M.; McCarthy, T.; Gottesfeld, S. *J. Appl. Electrochem.* **1993**, *23*, 86.